Proceedings ICFDP7:
Seventh International Congress on Fluid Dynamics and Propulsion
18 – 20 December 2001, Cairo, Egypt

ICFDP7-2001028

DEVELOPMENT AND CHARACTERIZATION OF A THERMAL FLOW SENSOR WITH A WIDE BANDWIDTH

A. Al-Salaymeh
Mechanical Engineering Department, University of Jordan, Amman, Jordan.
e-mail: salaymeh@ju.edu.jo

F. Durst
Lehrstuhl für Strömungsmechanik, Universität Erlangen-Nürnberg, Erlangen, Germany.
e-mail: durst@lstm.uni-erlangen.de

M. Gad-el-Hak
Department of Aerospace and Mechanical Engineering, University of Notre Dame, Notre Dame, IN, USA.
e-mail: gadelhak@nd.edu

ABSTRACT

Thermal flow sensors with a wide dynamic range are at present not available in spite of the large demand which exists for such sensors in practical fluid flow measurements. In this paper, it is shown that the velocity range of a "time-of-flight" thermal flowmeter for slowly changing flows can be increased by using wires (or other heating/sensing elements) with large thermal inertia (time constant) and heating the sending wire with a continuous sinusoidal current, instead of discrete, very short, square-wave pulses as in the usual pulsed-wire anemometer. The device described here uses two parallel wires of 12.5 μm diameter and its usable speed range is 0.05 to 25 m/s.

1. INTRODUCTION

Thermal sensors are widely applied in fluid flow measurements to yield local velocity information and also for volume flow-rate measurements. One subgroup of these sensors utilizes the convective heat loss as the basis of fluid velocity measurements. Hot-wire and hot-film anemometers are typical representatives of this subclass of thermal flow sensors, e.g. [1]. They are usually operated under constant temperature (CTA) or constant current (CCA) conditions and are also employed for flow-rate measurements in a wide range of applications, e.g. [2]. As far as their basic principles are concerned, thermal heat loss sensors can be taken as being fully developed. However, there are still interesting papers appearing in the literature showing new developments for special applications.

There are also many publications and patents which apply to a second subclass of thermal sensors for velocity measurements. These are concerned with a type of sensor that uses two wires mounted perpendicular to the flow to carry out "time-of-flight measurements" which yield velocity information. Sensors of this kind operate with the first (upstream) "sending" wire as an electrically heated device providing the flow with a time-varying thermal signal. This resultant thermal signal is convected downstream to the second "receiving" wire, which operates as a resistance thermometer, and detects the delayed arrival of the thermal signal.

The measured time of flight and the known distance between the sending and receiving wires permit the flow velocity to be computed. Hence, in principle, the operation of this type of thermal sensor is simple and the resultant response curve can be obtained as

$$\Delta t_f = \frac{\Delta x}{U} \qquad (1)$$

where Δx is the distance between the hot wires and U is the flow velocity. As experiments show, however, the measured time Δt_m is considerably longer than the above-given time of flight Δt_f. This is indicated in Fig. 1, which shows the differences that were obtained by the authors for a wire arrangement such as that at the top (right-hand side) of this figure with Δt = 1.5 mm. To explain the difference, it was suggested that the thermal time response of the finite-diameter sending and receiving wires could be responsible for the above-mentioned measured deviations. The time-constant results for hot-wire anemometers have been reported in the literature, e.g.

[3]. It also appears that these sensors are limited to a velocity range of roughly 1:20 or even less. Hence no sensors with wide dynamic ranges are available, e.g. sensors with a range of 1:500 which, at the same time, permit measurements at very low velocities of $U \leq 0.1$ m/s. These findings inspired the authors' investigations into wide-velocity range thermal sensors with an emphasis on the low-velocity end, and the outcome of this work is summarized in this paper.

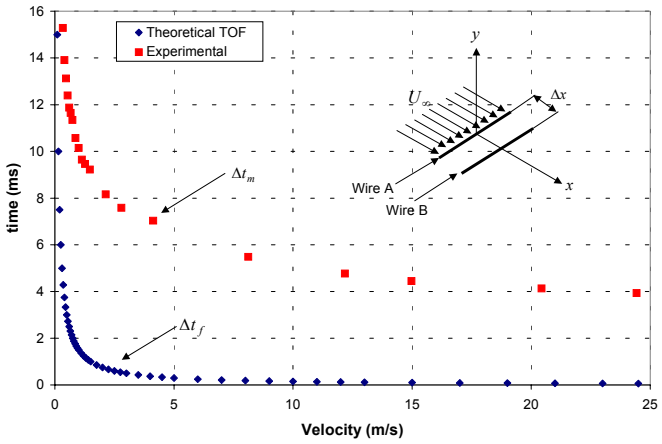

Fig. 1: A comparison between the theoretical time-of-flight and the measured time.

The first record found by the authors of the use of the pulsed-wire technique with square-wave pulses is the work of Bauer [4], who used two parallel wires for measurements in a laminar flow. The pulsed-wire anemometer technique was analyzed in detail by Bradbury and Castro [5]. The dynamic range of the flow velocity in the experiment of Bradbury and Castro was only about 14. On the other hand, the range of velocities possible with the pulsed-wire anemometer of Bradbury [6] was from 0.25 to 15 m/s and therefore its maximum dynamic range did not exceed 60. Tombach [7] performed his experiment at moderate and high flow velocities, so the minimum velocity was 1.3 m/s and the dynamic velocity range was about 60. This range represents the greatest speed range which was found in our literature survey.

2. SINUSOIDALLY-HEATED FLOWMETER

The present paper considers only the case of sinusoidal heating current. Also, it discusses only two-wire probes, with the two wires parallel. Our immediate application is to measurements of volume flow rates in slowly-changing unidirectional internal flows, which is why we call the device a "flowmeter" even though the primary response is to velocity.

The main finding is that the influence of the wire time constants on the calibration can be beneficial. Briefly, time constants decrease as the flow speed increases, so the total phase shift decreases more rapidly than if the time constants were negligibly small. This means that the speed range over which useful signals are obtainable is increased. The acceptable range for our probe is about 0.05 m/s to 25 m/s, a ratio of 1:500. Collis and Williams' empirical criterion for negligible buoyancy effects, that the Grashof number should be less than the cube root of the Reynolds number, suggests that buoyancy would become important only below 0.04 m/s, below the bottom of our usable range. For our conditions we found that the optimum wire diameter was about 12.5 μm (a standard size for commercially-available platinum wire) with our chosen heating-current frequency of 30 Hz and a wire spacing of 1.5 mm. There seems to be no advantage in using different diameters for the sending and receiving wires. Clearly this is not intended to be a fast-response device, but in principle similar probes with thinner wires, smaller spacing and higher excitation frequency could be made. For industrial or medical use, of course, thicker wires make a more rugged instrument. More details of our work are given in Durst et al. [8] and in Al-Salaymeh [9].

3. THEORETICAL INVESTIGATIONS

The total time lag or phase shift between the current to the sending wire and the temperature of the receiving wire, which acts as a resistance thermometer, is made up of (1) the thermal lag of the sending wire, (2) the true time of flight (convection by the fluid in the wake of the sending wire, with some effect of longitudinal heat diffusion at low speeds, and (3) the thermal lag of the receiving wire. The authors have made numerical calculations of all three over a range of parameters, taking account of variations of wire and fluid properties with temperature.

3.1 Response of the Sending Wire

The basic wire arrangement chosen by the authors for their theoretical investigations of a wide-range fluid-velocity sensor is sketched in Fig. 1. The sending wire, denoted wire A in Fig. 1, was assumed to be heated by a sinusoidally varying electrical current:

$$I(t) = I_0 + \Delta I \cdot \sin(2\pi f t) \qquad \textbf{(2)}$$

The final differential equation that describes the temperature of the sending wire is

$$\frac{dT_w}{dt} = \frac{I^2 \chi_\infty}{A_w(\rho_w c_w A_w)} + \left\{ \frac{I^2 \chi_\infty \alpha_\infty}{A_w(\rho_w c_w A_w)} - \frac{\pi k_f Nu}{(\rho_w c_w A_w)} \right\}(T_w - T_\infty) \qquad \textbf{(3)}$$

where Nu is Nusselt number for which Collis and Williams [10] found by experiment the relation

$$Nu = \left[0.24 + 0.56\,Re^{0.45}\right] \cdot \left[\frac{T_f}{T_\infty}\right]^{0.17} \qquad \textbf{(4)}$$

where Re is the wire Reynolds number, $Re = U d_w/\nu$. All fluid properties are calculated at the film temperature $T_f = (T_w + T_\infty)/2$.

This differential equation needed to be solved to yield the wire temperature as a function of time for given wire properties, a given fluid velocity and the time-varying electrical current. Fig. 2 shows that a distinct phase difference occurs between the current that drives the heating of the wire and the resultant temperature variation of the wire at low flow velocity $(U_\infty = 0.5 \text{ m/s})$. The temperature signal must be slightly non-sinusoidal because of variation of fluid and wire properties with time. The time difference between the two signals is a function of the flow velocity as indicated in Fig. 3.

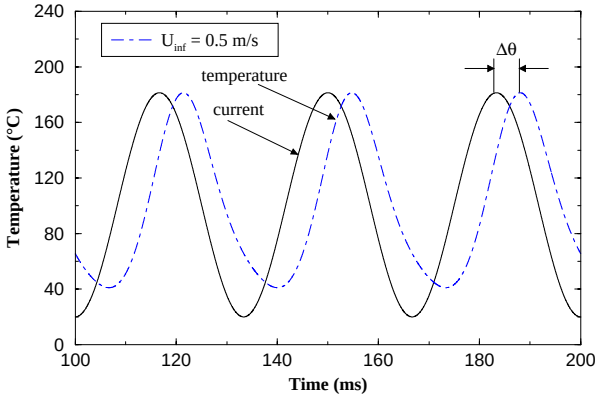

Fig. 2: The phase difference between the driving current signal and the output wire temperature at low flow velocity.

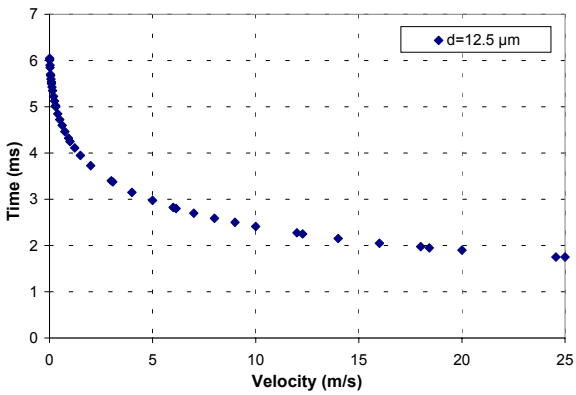

Fig. 3: The time difference between the driving current and the output temperature of a wire of 12.5 μm diameter as a function of flow velocity.

3.2 Time-of-Flight Calculations

In order to compute, from the calculated temperature variation of the sending wire, the resultant temperature variation of the fluid at the position of the receiving wire, denoted wire B in Fig. 1, the governing two-dimensional partial differential equations were solved.

Direct numerical simulations were carried out to estimate the temperature distribution around the sending wire, and especially at the receiving wire. The time lag between the sending temperature signal and the temperature signal at the receiving-wire position is calculated to give the time of flight. Fig. 4 shows typical results for the sending wire signal and the temperature signal at a certain downstream distance (say, 1.50 mm) and at a certain value of Reynolds number $(Re = 0.5)$ for a 12.5 μm wire diameter and for ambient temperature equal to 20 °C. As shown in Fig. 4, the amplitude of the downstream heated tracer is very small at the receiving-wire position compared with the sending signal. The time of flight can be simply calculated from the time lag between the two signals. Fig. 5 represents the computation results of the time of flight as a function of the free stream velocity based on a 12.5 μm heated wire diameter. The time delays due to the wire time constants are not included in these figures. Fig. 5 shows clearly that the dynamic range of the flow velocity obtained by time of flight alone is too limited.

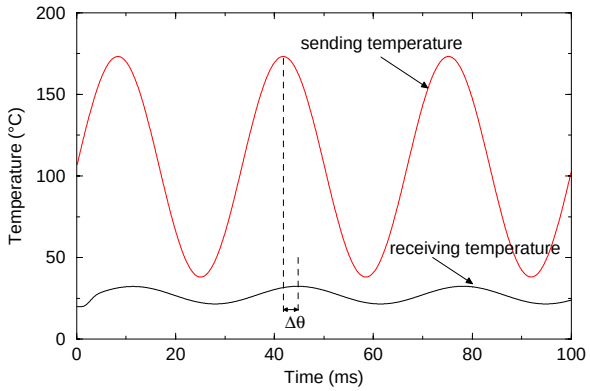

Fig. 4: The phase difference between the sending temperature of wire A and the fluid temperature at wire B. The time delays due to the wire time constants are not included.

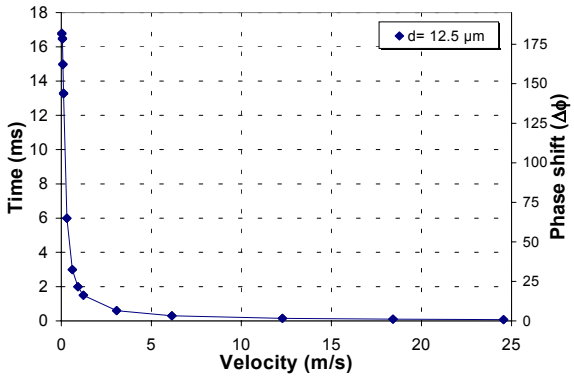

Fig. 5: Fluid time of flight versus the flow velocity. The time delays due to the wire time constants are not included.

3.3 Response of the Receiving Wire

The ambient fluctuation temperature, which is detected in the heated wake by the receiving wire, has an approximately sinusoidal shape. A very small, constant current passes through the receiving wire so that its resistance (temperature) can be measured, but its heating effect can be neglected. Therefore,

the thermal energy balance for the receiving wire can be written as

$$\frac{dT_w}{dt} = \frac{\pi Nuk_f}{(\rho_w c_w A_w)}(T_a - T_w) \quad \textbf{(5)}$$

Equation (5), which is a first-order ordinary differential equation, can be integrated with respect to time to obtain the receiving wire temperature fluctuation in the following form:

$$T_w = T_m + \left(\frac{\Delta T_a}{1+\omega^2 M^2}\right)\left[\cos(\omega t) + M\omega \sin(\omega t)\right] + C_1 e^{-\frac{t}{M}} \quad \textbf{(6)}$$

where C_1 is the integration constant which satisfies the initial condition and M is the wire time constant:

$$M = \frac{\rho_w c_w A_w}{\pi Nuk_f} \quad \textbf{(7)}$$

Different flow velocities were substituted in equation (6), as represented by different values of *Nu* in equation (7), to yield the receiving-wire temperature variations with time. Fig. 6 shows the time lag or the phase difference that occurs between the fluctuating ambient temperature in the heated wake of the sending wire and the resultant temperature variation of the receiving wire. This corresponding time difference is a function of the flow velocity as indicated in Fig. 7.

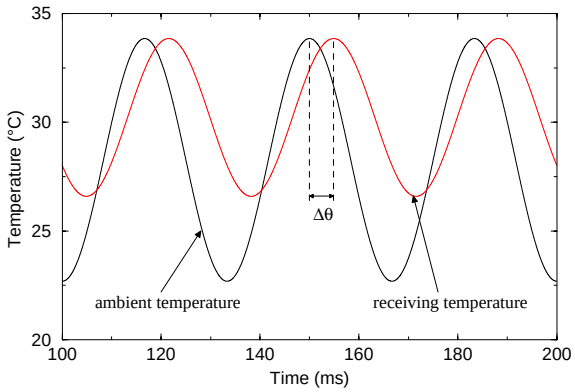

Fig. 6: The phase difference between the ambient temperature signal in the heated wake and the output temperature signal at the receiving wire.

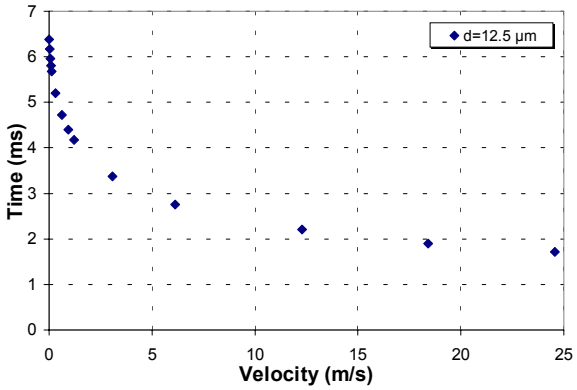

Fig. 7: The time difference between the ambient temperature signal in the heated wake and the output temperature of receiving wire of a 12.5 μm diameter as a function of flow velocity.

Fig. 8 shows the values of the time shift between the sending and the receiving signals obtained from the theoretical results on the basis of the present observations. This time shift represents the summation of the three time difference components: the time lag of the sending wire, the time of flight, and the time lag of the receiving wire, which represents the theoretical behavior of our thermal sensor.

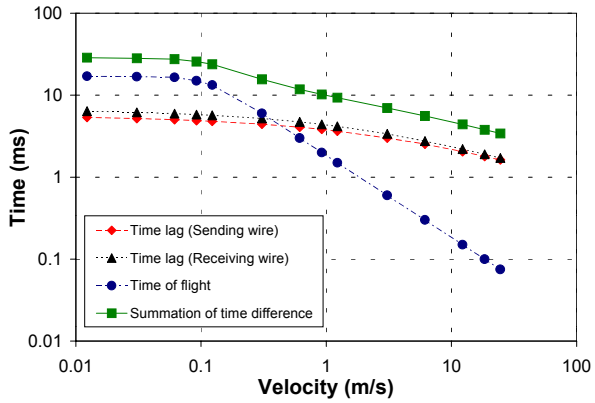

Fig. 8: The three components of the time difference and their summation versus the flow velocity (log scales).

4. SELECTION OF SENSOR PARAMETERS

4.1 Driving Current Frequency

The maximum permissible frequency, *f*, of the driving current must be an order of magnitude lower than the reciprocal of the sending wire time constant, to avoid severe attenuation of the temperature variation in the sending wire. Therefore, the maximum current frequency can be expected to be of the order of 100 Hz or less than this value.

The strong dependence of amplitude of the sending wire output temperature signal on the driving current frequency at a given velocity is shown in Fig.9. The magnitude of the temperature fluctuation of the wire is less than the magnitude of the forcing

input signal by the factor $1/\sqrt{(1+M^2\omega^2)}$. In addition, the temperature response of the sending or receiving wire is shifted in phase with respect to the forcing function by an amount depending upon the time constant and the frequency as shown in equation (8):

$$\Delta\phi_{shift} = \omega\,\Delta t_{shift} = \arctan(M\omega) \qquad \textbf{(8)}$$

It is recommended that one should obtain an output temperature signal with large amplitude to extend the dynamic range of the sensor. Therefore, it is essential that the current frequency of the sending wire be as small as possible. Also, it is noted that the sending-wire phase shift does not matter (much), so all that is needed is for $1/\sqrt{(1+\omega^2M^2)}$ to be not too small compared with unity; 0.7 would be acceptable and one can obtain that with $\omega M = 1$, a frequency of 30 Hz which is suitable for the application of the present sensor to tasks such as the measurement of breathing of animals.

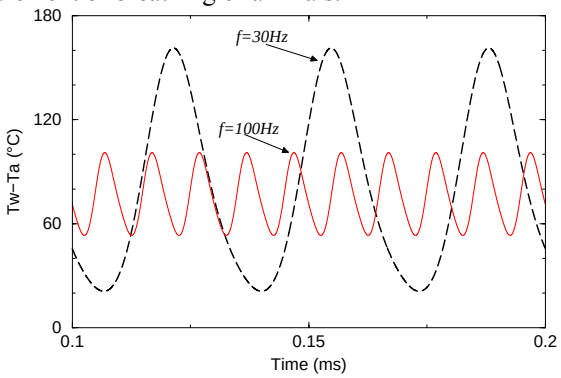

Fig. 9: The response of the sending wire to varying frequencies of a supply current is plotted as ΔT (°C) versus time (*ms*).

4.2 Time Constant of the Sensor Wires

The temperature response "output" of each wire is shifted in phase with respect to the "input" signal, i.e. the heating of the sending wire by the electrical input and of the receiving wire by the thermal wake, by an amount that depends on the wire time constant and the current frequency (see equation (8)). It should be pointed out that the phase shifts for the sending and receiving wires are in close agreement, but for low flow velocity the time lag of the sending wire is slightly lower than that of the receiving wire. Fig. 10 represents the phase difference between the input and output signals as a function of the flow velocity. This figure demonstrates the increase in the value of the time constant when the diameter increases. The results show that the time shift decreases with increasing velocity because *Nu* increases with *Re* as shown in equation (4), and the time constant is inversely proportional to *Nu* as predicted by equation (7). An increase in the wire diameter enhances the dynamic range of the present thermal sensor. However, an increase in the wire diameter to a high value (say 25 μm) has an adverse effect. As shown in Fig. 11, 12.5 μm is an optimum value that has a high dynamic range (the maximum time lag divided by minimum time lag) and its sensitivity is very good over all the velocity range.

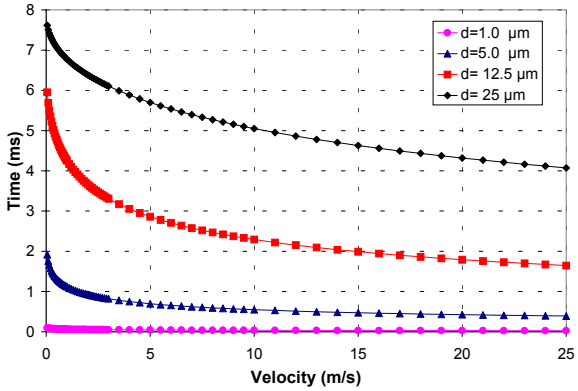

Fig. 10: The phase difference between the wire "input" and "output" signals (as defined in the text) versus the flow velocity for different diameters.

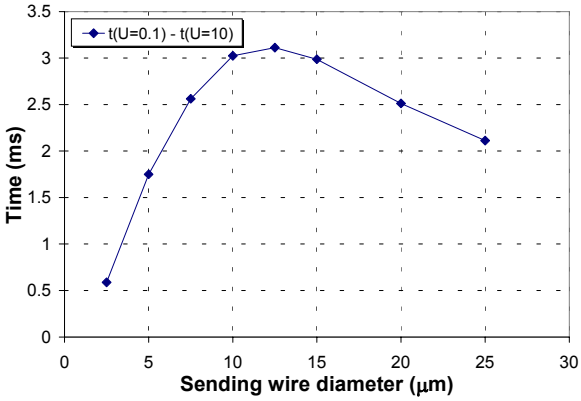

Fig. 11: The change in time difference over a given change of velocity $(0.1\ \text{m/s} \le U_\infty \le 10\ \text{m/s})$ versus wire diameter.

4.3 Time-of-Flight Component

The phase shift between the sending and the receiving temperature signals at a certain downstream distance is computed to obtain the time of flight. It was found that the solution to the two-dimensional energy equation for convection and diffusion of heat in a laminar stream is a strong function of the Peclet number. The Peclet number ($Pe = Re \cdot Pr$, where *Re* depends on the distance Δx between the two wires) can be interpreted as the ratio between the diffusion time ($\Delta x^2/a$) and the convection time ($\Delta x/U$), where *a* is the thermal diffusivity of the fluid $(a = k/\rho c_p)$. If the Peclet number is less than 50 (a flow speed below 0.7 *m/s* with $\Delta x = 1.5\ mm$, our preferred value), the diffusion effect will be noticeable, and this effect will increase too much when the Peclet number decreases to 10. Fig. 12 shows the relation between the Peclet number and the detected time of flight. However, as the velocity is increased, the diffusion effect rapidly becomes negligible compared with the convection time and the wire time constant.

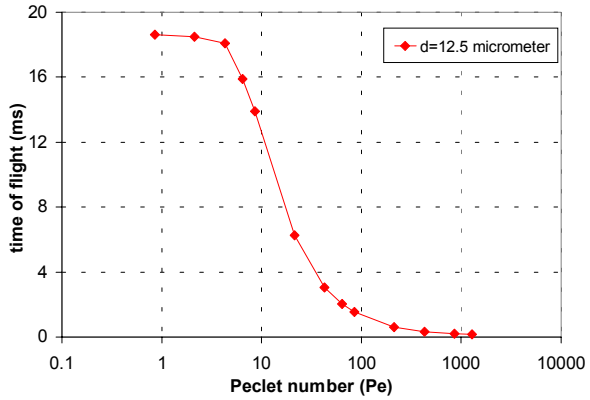

Fig. 12: The detected time of flight as a function of Peclet number at $\Delta x = 1.5$ mm.

4.4 Effect of Ambient Temperature Variations

Numerical calculations were carried out to study the influence of ambient temperature variation on the summation of the time difference between the sending and receiving signals. Fig. 13 shows that there is a very small effect of ambient temperature variations on the results. The time constant of both wires was found to decrease slowly with increasing the ambient temperature. The time-of-flight component can be accurately found to be independent of the ambient temperature over a wide speed range except at very low flow velocities at which the diffusion time is dominant. The summation of the time lag due to the time constant of the sending and receiving wires in addition to the time of flight are presented in Fig. 13. The influence of the ambient temperature variation can be seen at very low velocities $(U_\infty \le 0.1\,\text{m/s})$ because of the serious effect of the diffusion. The diffusion time is inversely proportional to the thermal diffusivity, which increases with temperature.

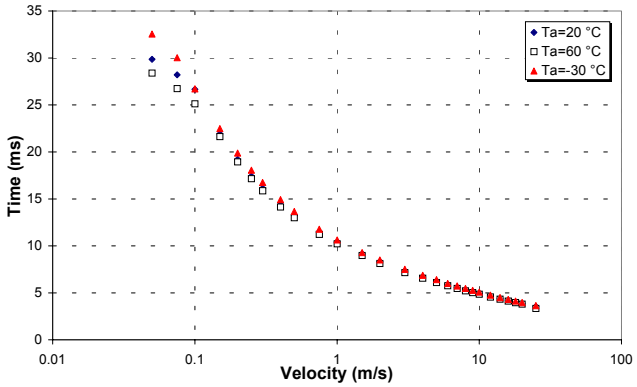

Fig. 13: Influence of ambient temperature variation (-30 to 60 °C) on the summation of the three time components.

5. Experimental Results and Comparisons

5.1 Sensor Calibration

Owing to the non-linear behavior of the thermal flow sensor, calibration over the whole speed range is necessary. Although in principle this is a disadvantage, it is at the same time an advantage to have a non-linear transfer function giving high accuracy at the lower end of the range, and thus to have approximately the same percentage accuracy over the whole range.

The mean-flow calibration obtained from the position of the wire intercepts of the thermal sensor (Δx = 1.5 mm) is shown in Fig. 14. The calibration data was carried out over the range from very low velocities (down to 0.05 m/s) to very high velocities (up to 25 m/s). The results show that the present sensor can cover the whole dynamic range of 500:1 with high accuracy and sensitivity.

One of the major problems with hot-wire anemometers is long-term stability. This is especially the case when the sensing element is made very small to give a fast time response. "Short-term" drift in the hot wire occurs as a result of air temperature changes and dirt accumulation and "long-term" drift results from metallurgical changes of the wire. It is well known from hot-wire anemometry that calibration of the wire is necessary at relatively short time intervals, perhaps several times a day. The reason for this is the relatively large change in heat exchange from the wire to the surroundings, when the ambient temperature drifts slightly or when the wire is contaminated. Even in environments with relatively clean gas contamination can occur. The described sensor does not suffer from this problem, because the principal operation of this probe depends on the phase shift between the sending and the receiving signals. To verify this statement, a number of tests were carried out. The same calibration results were maintained after several days of operation with an error of less than 3%. Fig. 14 demonstrates the independence of the calibration curve for the present sensor on the outside conditions and its repeatability. Also, one can conclude from Fig. 14 that the repeatability of this sensor is very high and therefore this device is sufficient for many applications.

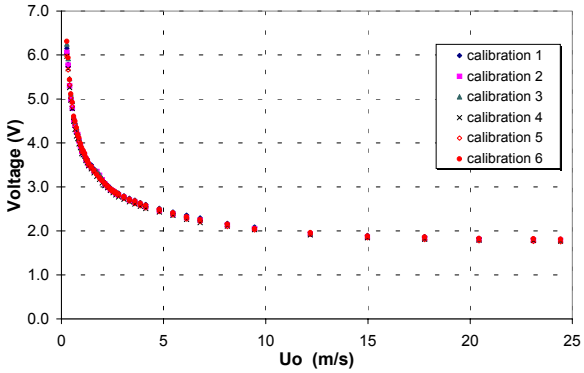

Fig. 14: The long-term stability of the thermal flow sensor.

5.2 Comparison of experimental and theoretical results

The experimental data were compared with the theoretical results derived in Section 3. The comparison shown in Fig. 15 indicates excellent agreement between the theoretical and experimental results over the whole dynamic range of the velocity flow.

The results showed that the time difference between the sending and receiving signals increases gradually at low velocities $(U_\infty \le 0.1\,\text{m/s})$. This behavior verifies the leading rule of diffusion in the case of low flow velocity. The dominance of diffusion over transport became more important as the velocity became weaker. Fig. 15 shows that the time shift between the sending and the receiving signals at $U_\infty > 0.1\,\text{m/s}$ is approximately inversely proportional to the one-third power of the flow velocity ($\Delta t \propto U_\infty^{-1/3}$), whereas the time-of-flight component is inversely proportional to the flow velocity ($\Delta t_f \propto U_\infty^{-1}$). Therefore, the dynamic range of the measured velocity by the present sensor is high and it is larger than that of the pulsed-wire anemometer, which measures only the time of flight to determine the flow velocity.

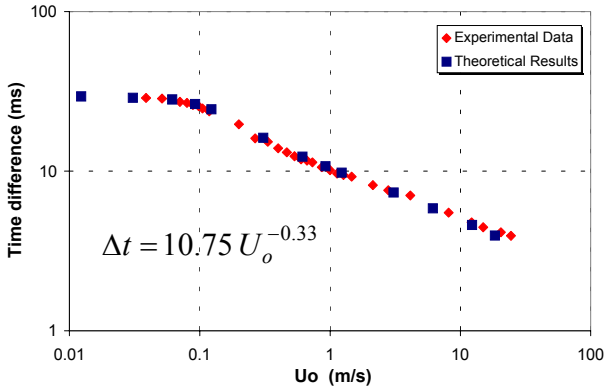

Fig. 15: Comparison between experimental and computed results for thermal flow sensor drawn on log scales.

6. CONCLUSIONS

The present paper described a novel instrument, a thermal flow sensor, that has been made for measuring a flow velocity under a wide variety of conditions over a large dynamic range. Its construction is such that it can be produced at a low cost for industrial applications. Also, this paper has presented the results of both theoretical and experimental investigations into this sensor using the technique of determining the time constants of the used wires parallel to the time of flight for velocity measurement.

The present sensor can measure mean velocity over a wide range (from 0.05 to 25 m/s). Therefore, the instrument has a very high dynamic range and flow rate variations in the range 1:500 are feasible. The computed results predicted by theory are globally confirmed and the agreement between the experimental and theoretical results is very good over the whole range. This sensor has some advantages such as a low sensitivity to variations in temperature and also to the composition of the flowing gas. The instrument is designed to measure time-varying flow rate with limited frequency ($f \le 30$ Hz). The addition of a second, upstream, receiving wire to the present probe allows to resolve a given velocity component irrespective of sign.

ACKNOWLEDGMENTS

The authors greatly appreciate the support received from the Lehrstuhl für Strömungsmechanik (LSTM), Friedrich-Alexander-Universität, Erlangen-Nürnberg. A. Al-Salaymeh was financially supported by DAAD (German Academic Exchange Service) when carrying out this research.

REFERENCES

[1] Perry, A. E. (1982) "*Hot-Wire Anemometry*," Oxford University Press, Oxford.

[2] Bruun, H. H. (1995) "*Hot-Wire Anemometry. Principles and Signal Analysis*," Oxford University Press, Oxford.

[3] Antonia, R. A., Browne, L. W. B., and Chambers, A. J. (1981) "Determination of Time Constants of Cold Wires," *Rev. Sci. Instrum.* **52**, 1382–1385.

[4] Bauer, A. B. (1965) "Direct measurement of velocity by hot-wire anemometry," *AIAA J.* **3**, 1189–1191.

[5] Bradbury, L. J. S. and Castro, I. P. (1971) "A pulsed-wire technique for measurements in highly turbulent flows," *J. Fluid Mech.* **49**, 657–691.

[6] Bradbury, L. J. S. (1976) "Measurements with a pulsed-wire and a hot-wire anemometer in the highly turbulent wake of a normal flat plate," *J. Fluid Mech.* **77**, 473–497.

[7] Tombach, I. H. (1973) "An evaluation of the heat pulse anemometer for velocity measurement in inhomogeneous turbulent flow," *Rev. Sci. Instrum.* **44**, 141–148.

[8] Durst, F., Al-Salaymeh, A. and Jovanović, J. (2001) "Theoretical and experimental investigations of a wide range thermal velocity sensor," *Meas. Sci. Technol.* **12** 223–237.

[9] Al-Salaymeh, A. (2001) "*Flow velocity and volume flow rate sensors with a wide band width",* Ph.D.

Dissertation, Technischen Fakultät der Universität Erlangen-Nürnberg.

[10] Collis, D. C. and Williams, M. J. (1959) “Two-dimensional convection from heated wires at low Reynolds numbers,” *J. Fluid Mech.* **6**, 357–384.